Measurements of Load Train Motion on a Stratospheric Balloon Flight

Timothy D. Gruner, David J. Olney, and Angela M. Russo

Final Review Copy

Figures are embedded from Paper_Figures.ppt

8/30/2005 3:33:39 PM

Measurements of Load Train Motion on a Stratospheric Balloon Flight

Timothy D. Gruner, David J. Olney, and Angela M. Russo
NASA Goddard Space Flight Center

Abstract
Attitude measurements using gyros and magnetometers placed on a stratospheric balloon during a non-pointed test flight were used to observe the natural azimuth and elevation motions of a balloon/load train/gondola at an altitude of 36 km over a total flight time of 400 minutes. Time traces of the entire flight are presented. This flight, conducted under nominal atmospheric conditions, had significant motion about the azimuth. Some discussion on balloon disturbances is also included.

Introduction

Unlike the situation with spacecraft, stratospheric balloon pointing systems need to contend with the fact that the gondola is attached to the balloon via a long flexible structure, called the load train. Besides transmitting the balloon's buoyant force, the load train is the source of disturbances that the pointing control system must reject. A typical stratospheric balloon 131 m (430 ft) in diameter has a load train 79 m (260 feet) in length comprised of an unpacked parachute beneath which is connected a cable ladder 20 m (65 ft). (Figure 1) The ladder serves to provide additional length to that of the parachute thereby increasing the unobstructed field of view upwards from the gondola. Comparatively shorter gondola-specific attachment cabling structures and balloon control electronics are also on the train.

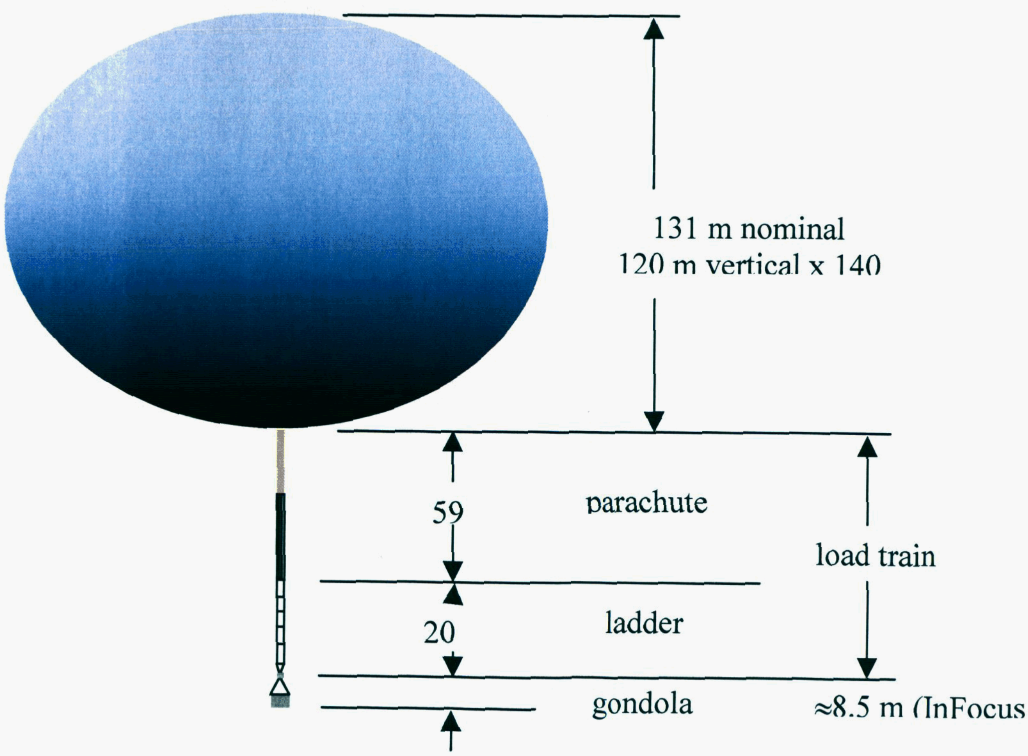

Figure 1 Stratospheric Balloon Configuration – Typical Sizes

The intent of this paper is to show measurements that were made using magnetometers and gyros on a balloon flight in August 2000. What makes the data unique is that three of the magnetometers were placed on the load train as discussed below. The primary mission of this flight was to perform background calibration on a detector module that was to be a critical part of a nine-meter long X-ray telescope. The telescope was being readied to make long observations at X-ray targets on a subsequent flight. The module on the flight discussed here was fixed to the gondola and did not require pointing. But the flight provided a timely opportunity to piggyback attitude instrumentation on the gondola and load train solely for observing their natural motion during the ascent and float phases of the mission. It was hoped that this information would be helpful in efforts to characterize disturbances that could be expected on any balloon-borne pointing system.

Pointing Disturbances

Whenever telescopes have been placed on balloon gondolas, the disturbances from the load train have been a significant concern in the pointing system design, especially as desired accuracies have progressed from degree to arcminute level. There are two categories of disturbances: transverse and azimuth. Transverse disturbances include "pendulous" swinging and "jangling" oscillations that mostly affect gondola (or telescope) rotations about the two horizontal axes (referred to here as the elevation and cross elevation axes). Azimuth disturbances are twisting-type disturbances about the vertical that similarly affect the gondola/telescope azimuth positioning.

Each science payload team devises methods for mitigating the effects of these disturbances. The primary strategy is to place the balloon in as quiescent an environment as possible during observation. Low winds at the float altitude (for mid latitudes) are sought by launching during the semiannual "turn-around", i.e., a several-week period in the spring and again in the fall where upper atmospheric (e.g. 35-40 km) winds gradually shift direction, passing through zero in the process. Regardless, the balloon must ascend through the troposphere and tropopause at a relatively high ascent rate to avoid excessive cooling of the balloon. The turbulence can excite the balloon/load train/gondola dynamics, which on arrival at the float altitude are manifested as oscillations that will disrupt pointing until they have dampened. Also, ballast drops occur on a regular basis causing sudden changes in altitude disturbing the static equilibrium of the flight configuration.

The second strategy is in the careful design of the pointing system. The most common pointing configuration is the azimuth/elevation configuration where the entire gondola is rotated about vertical while the telescope is tilted about a horizontal elevation axis fixed in the gondola. To observe celestial targets from a balloon, both elevation and azimuth (measured with respect to north), must vary over time. Ideally, the telescope body is rotationally isolated from the gondola base and balanced with its center of mass close to its center of rotation, so that disturbance torques are not generated from transverse accelerations. It is also ideal to provide control torques that do not react with the gondola base, e.g., reaction wheels, magnetic torque coils, or gas thrusters. If the telescope is rotated in elevation by a mechanism that does react with the gondola base the rotation needs to be done gently, otherwise there is a risk of rocking the gondola and exciting transverse modes in the load train. It is commonly known that the dominant natural transverse oscillations of the balloon/load train/gondola exist with both long (e.g., ~ 30 second) and short (e.g., ~ 3 second) periods.

About the vertical axis, natural motion in azimuth is less obvious. The top of the load train, i.e., the parachute is attached to the bottom of the balloon with a hook. This constrains the load train to more or less match the azimuth rotation of the balloon. It is not obvious how the balloon is going to rotate during a flight, if at all. At first, one might expect the balloon rotation to be negligible at float altitude since it is launched with a small volume of gas that expands during ascent creating a much higher moment of inertia (~ 10^6 kg-m^2). But the effects of aerodynamics on a balloon are not negligible and balloon rotation even during float has been noted in the past. This uncertainty was another reason why measurements were being made.

Gondolas requiring azimuth control are attached to the bottom of the load train using a low friction decoupler, designed for unlimited rotation. The gondola is usually rotated with a reaction wheel avoiding disturbances into the load train. However, some friction is always present.

With some decoupler mechanisms the friction can be increased in a controlled way and the torque applied against the load train is then used for reaction wheel unloading. However, reacting against the load train as the sole means of azimuth control and slewing is not considered workable because of the low compliance of the ladder and parachute. In other words, a significant amount of rotation of the load train is needed in order to achieve an acceptable torque.

Load Train Description

Referring to Figure 2, the hook at the termination fitting (at the top of the load train) is attached via short cables to a ring that is equal in diameter to the hole at the center of the parachute canopy. From this ring the parachute hangs for about 60 m (195 feet). At the bottom its shroud lines are attached to a similarly sized ring so that under tension during flight, the parachute clearly becomes a torsion pendulum. A short distance below the lower ring, connected via a short set of cables structure, is the top of the ladder. Metal cables form the sides of the ladder running for 20 m (65 ft). The cables are kept spaced by rigid rungs every 3 m (10 ft). The cable spacing makes the ladder another torsion pendulum. Cables at the bottom of the ladder come together to a fixture used to hold the gondola during its launch from a mobile launcher. Below the fixture is the decoupler and then the gondola structure.

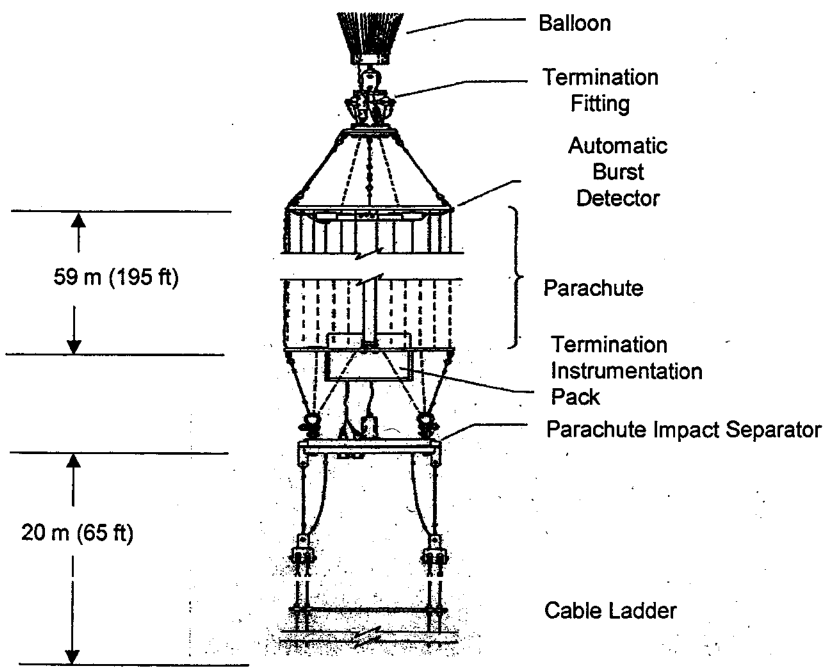

Figure 2 NSBF Drawing of the Standard Load Train Elements

Prior to the flight, the National Scientific Balloon Facility (NSBF) loaned a ladder to the InFocus team at the Goddard Space Flight Center (GSFC) in order to study its dynamic characteristics. It was suspended in a high bay under a 1000 kg load to observe the nature of its movement as shown in Figure 3. In both azimuth and elevation, the ladder was observed to move with highly complex oscillations suggesting that the structure behaves not unlike waves traveling along a string under tension. Traveling waves moved up and down its length, presumably completely reflected from its rigid attachment at the ceiling. It was hoped that the measurements on the flight would shed light on the dissipation of these waves when the ladder is attached to a more compliant parachute and balloon.

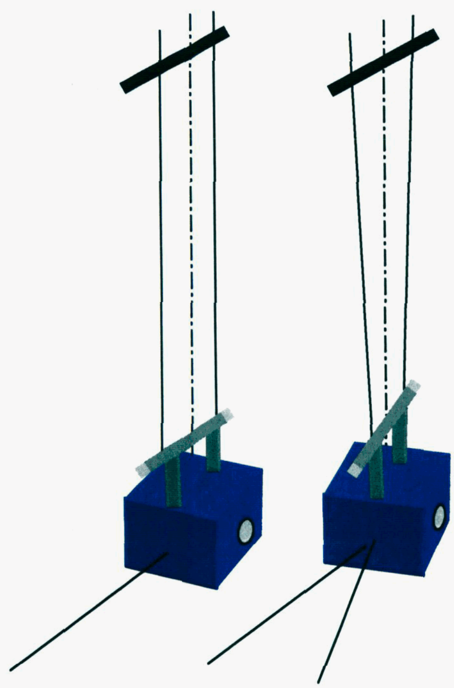

Figure 3 Illustration of the torsional azimuth motion of the ladder under a test load

Instrumentation

With no requirement to point the gondola on this flight, a decoupler between the gondola and load train was not included. This allowed signal cables to be run from magnetometers along the ladder to the gondola where the data system and transmitters were located. Three magnetometers were placed along the ladder at the three stations as shown in figure 4. A fourth magnetometer was attached to the gondola. Two of the four magnetometers, at the top and on the gondola, were three-axis magnetometers while the remaining two were two-axis magnetometers with both their sensing axes placed in the horizontal plane. The top magnetometer was attached to the ring at the top of the parachute. The remaining intermediate magnetometers were mounted to ladder rungs.

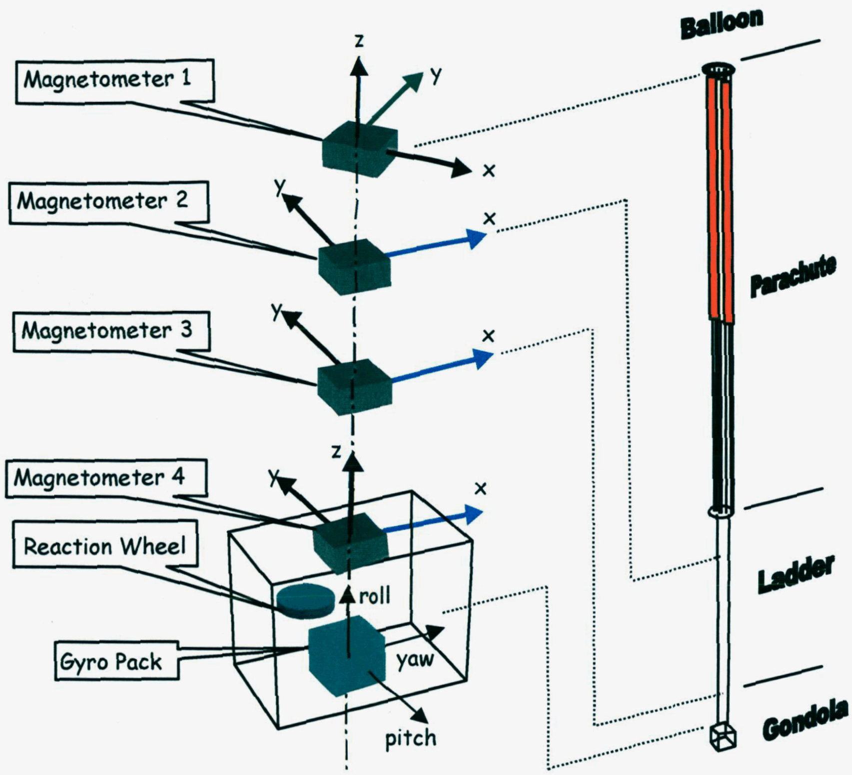

Figure 4 Arrangement of Sensors and their Locations on the Load Train

The three lower magnetometers were aligned by virtue of the ladder attachment to the gondola. For operational reasons, the alignment (about the vertical) of the top magnetometer with respect to the remaining three could not be measured before launch and was inferred from the post flight data.

A three-axis gyro package was carried on the gondola. The package was capable of integrating the gyro rate signal of all three channels within +/- 10 degrees. Finally a reaction wheel was placed on the gondola with its spin axis vertical. The reaction wheel was included to provide a method to excite azimuth motion during flight. The wheel had a peak torque capability of 30 newton-meters.

Flight

The payload was launched in the early evening on August 29, 2000 at 7:30 CDT from the NSBF facility at Palestine, Texas. The weather conditions were clear with no significant surface or high altitude winds. The time from launch to parachute separation was approximate 400 minutes, a short flight compared to most pointed observation flights. Data was telemetered to the ground via a UHF link. The float altitude was nominally 36 km, maintained by occasional dumping of ballast. See Figure 5. At this altitude the atmospheric density is quite low, approximately 0.007 kg/m^2 or 0.6 % that of sea level. The overall horizontal velocity of the flight averaged 40 knots.

Prior to termination of the flight, the reaction wheel in the gondola was operated in order to observe its effect on azimuth motion. The flight was terminated for landing zone considerations.

This precluded an opportunity to observe effects caused by altitude variations at sunrise as the sun illuminated the balloon.

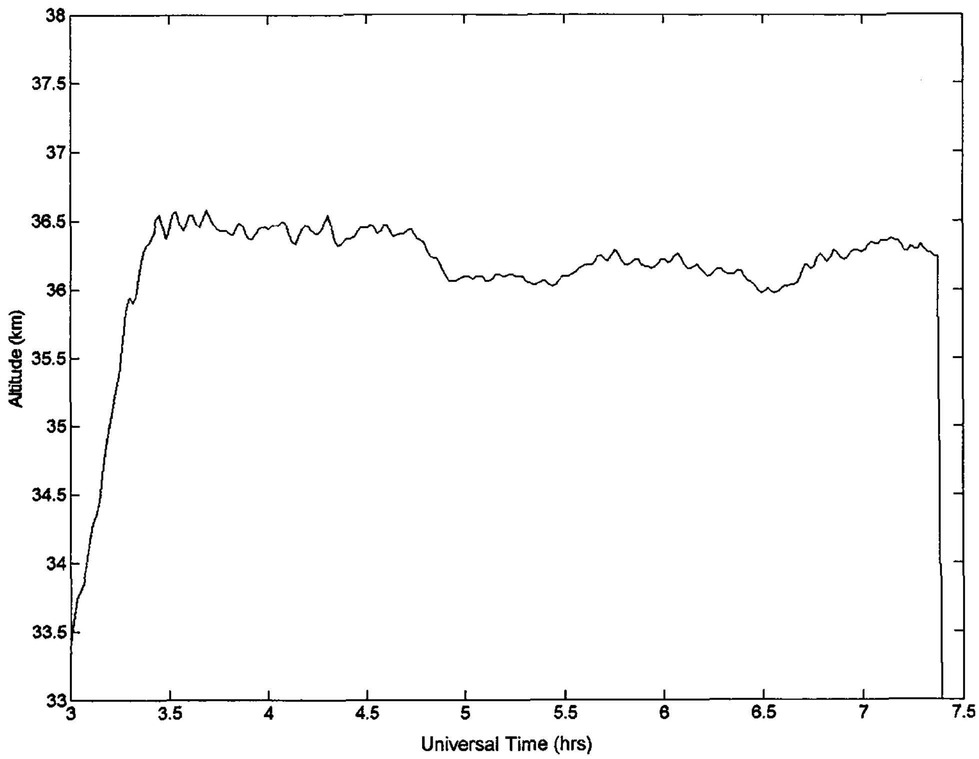

Figure 5 Altitude (km) as measured by NSBF during the floated phase of flight

Flight Results

A section of the data from approximately 4 hours after launch (note: time scale in seconds) is shown in Figure 6. Shown are sensor outputs when the gondola is completing ascent and settling at the float altitude of approximately 36 km. It is obvious in the first chart (gyro rate) and second chart (gyro integrated rate) that the transverse motion in elevation and cross elevation are small compared to azimuth.

The gyro- integrated rate frequently saturates in the roll channel (azimuth) as was expected.

The magnetometer channel data are grouped by magnetometer axes. Subplot 3, for example, has all the X axes of figure 4. The Z channels on subplot 5 show very little movement implying that the elevation was not greatly perturbed.

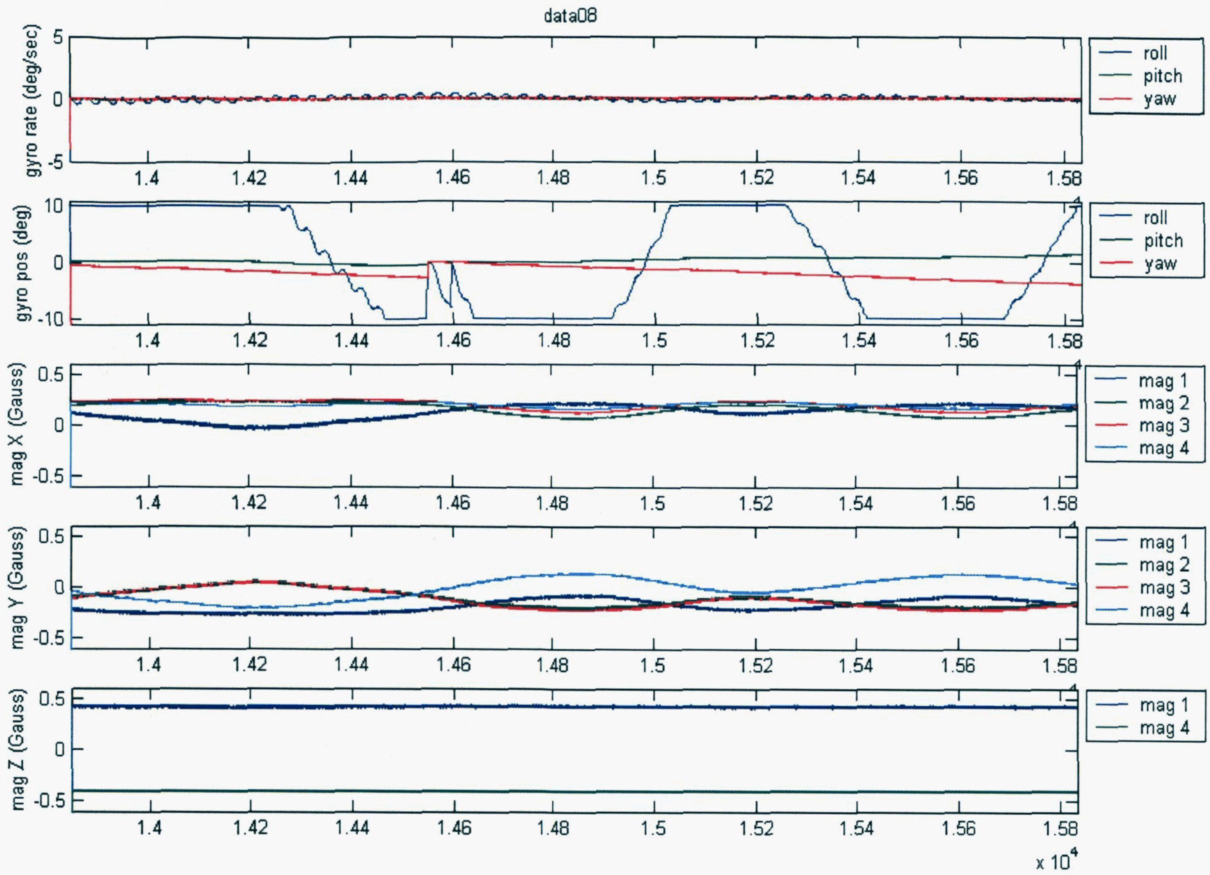

Figure 6 Representative Data Set for Measurements of Load Train Motion on a Stratospheric Balloon Flight; gyro rate, mag X, mag Y and post-flight calculated azimuth or mag Z, versus approximate elapsed time from launch (seconds).

Observations

In the appendix, the data throughout the entire flight is shown. This includes gyro rate and the magnetometer readings as well as the azimuth from magnetic North, which was computed post flight from the magnetometer readings.

Each set of graphs covers 2000 seconds of flight time. T=0 occurs at gondola release from the NSBF mobile launcher "Tiny Tim" when the balloon, having been released a few seconds earlier, had ascended sufficiently high to lift the gondola/load train. The first subplot shows the three gyro rate channels. The second shows the X channels for the four magnetometers and the third graphs shows the Y channels.

The fourth graph shows the azimuth of each magnetometer measured from magnetic north using the transverse magnetometer channels. The azimuth angle was calculated post flight from the magnetometer data using a Matlab atan2 function. For visual clarity the azimuth is often allowed to increase in range beyond 0 to 360 degrees. Occasional discrete changes in the data are the result of telemetry dropout.

Elevation

The elevation rate vs time shows damping of the gondola rate during the floated phase. There are times when the elevation rate increases, although no actuators are operating on the gondola. During the float, ballast drops are commanded by the NSBF, which along with atmospheric disturbances is a possible source of elevation excitation. Figure 7 shows the elevation rate throughout the entire flight.

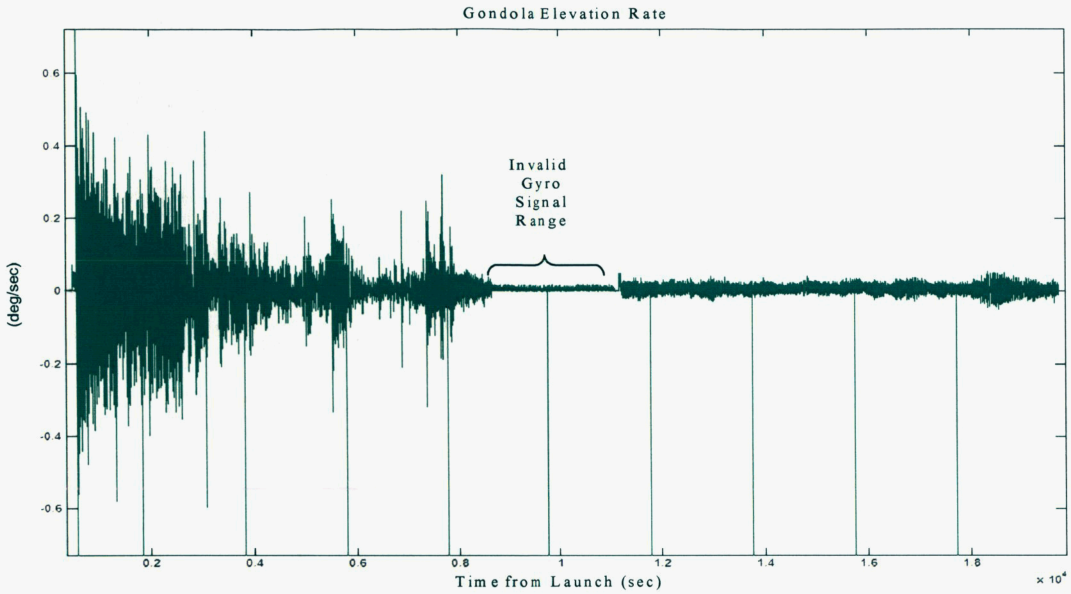

Figure 7 Unfiltered Elevation Rate

A detailed segment of the above elevation motion reveals the multiple frequency nature of the elevation motion as shown in Figure 8. The sampled data points are indicated. Figure 9 shows the multiple frequency nature of elevation and cross elevation.

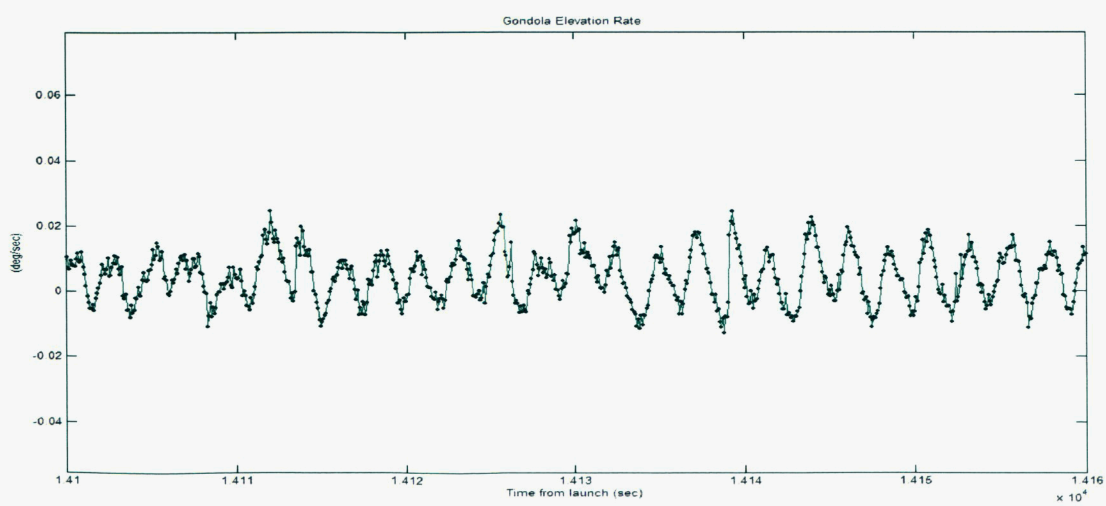

Figure 8 The gondola rate during the float phase about the elevation axis over one minute

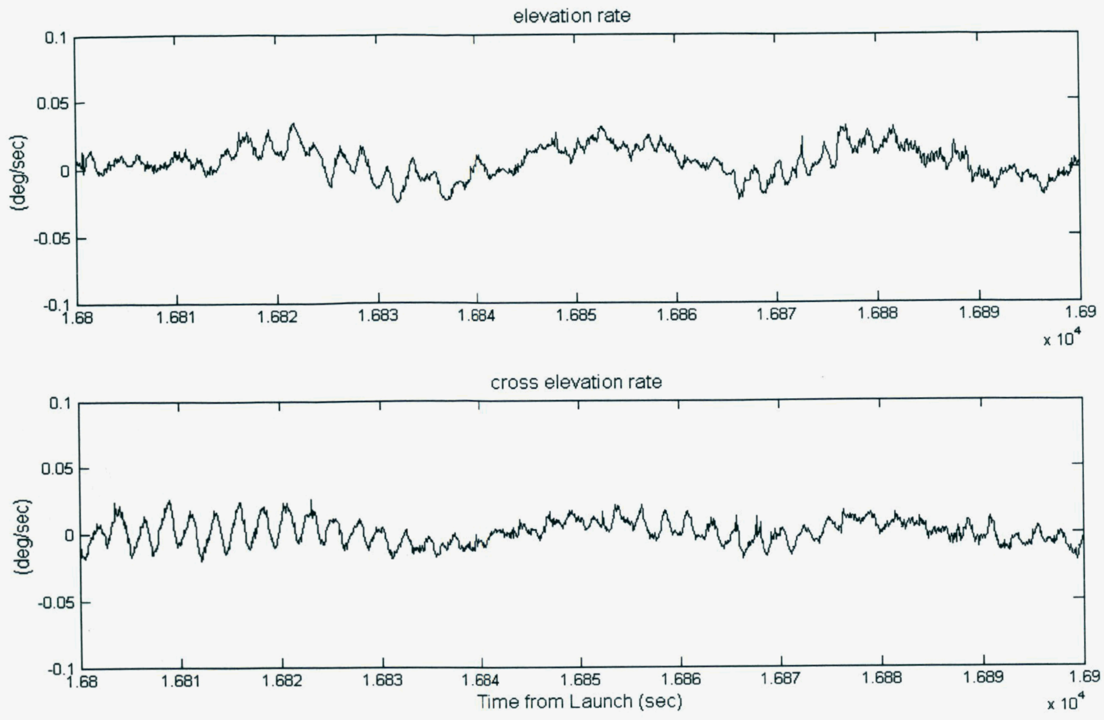

Figure 9 Multiple Frequencies on Elevation and Cross Elevation Rate

Azimuth Results

The change of the balloon azimuth can be visualized on a cylindrical surface as in Figure 9 where time increases in height. The output is derived from magnetometer 1 which was mounted to the upper parachute ring just below the balloon hook.

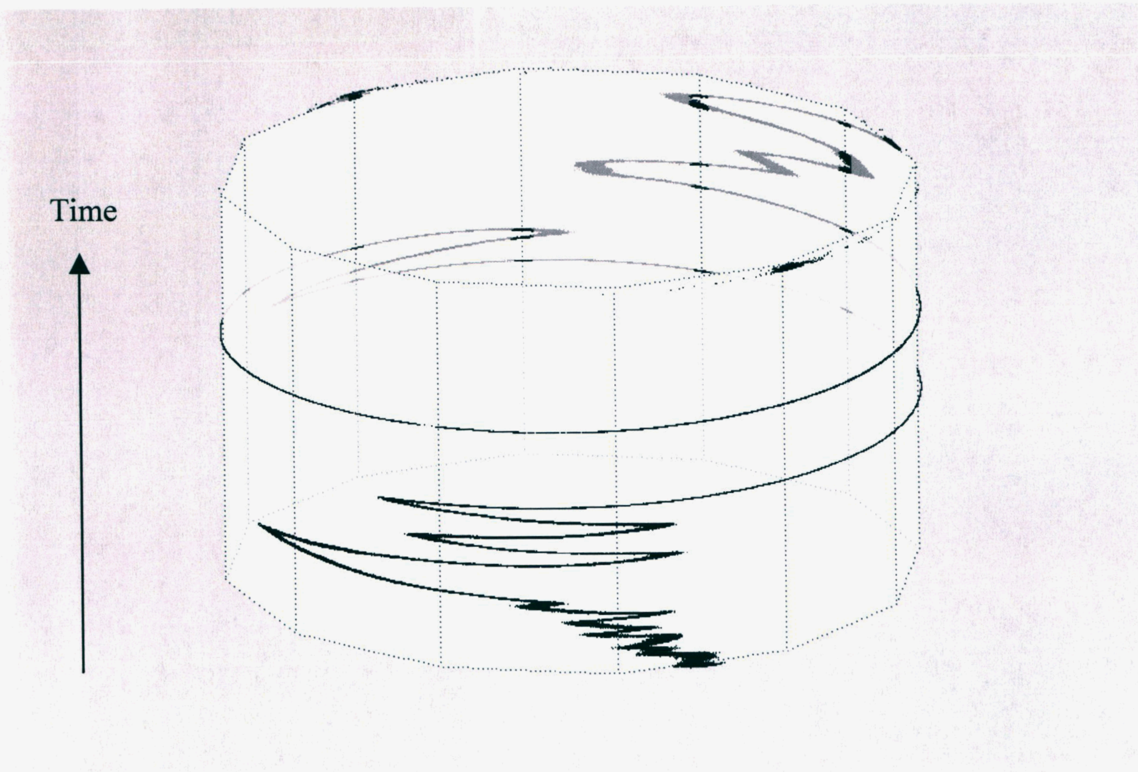

Figure 10. Azimuth rotation of the balloon from 8000 seconds to 20000 seconds as measured with magnetometer 1

Filtered Azimuth Data

Figure 11 shows the results from all four magnetometers after their computed azimuths were filtered with a band pass .012-5 Hz, over a shorter time range time of 10000 to 12000 seconds from launch and for a shorter time period, 400 sec, in Figure 12.

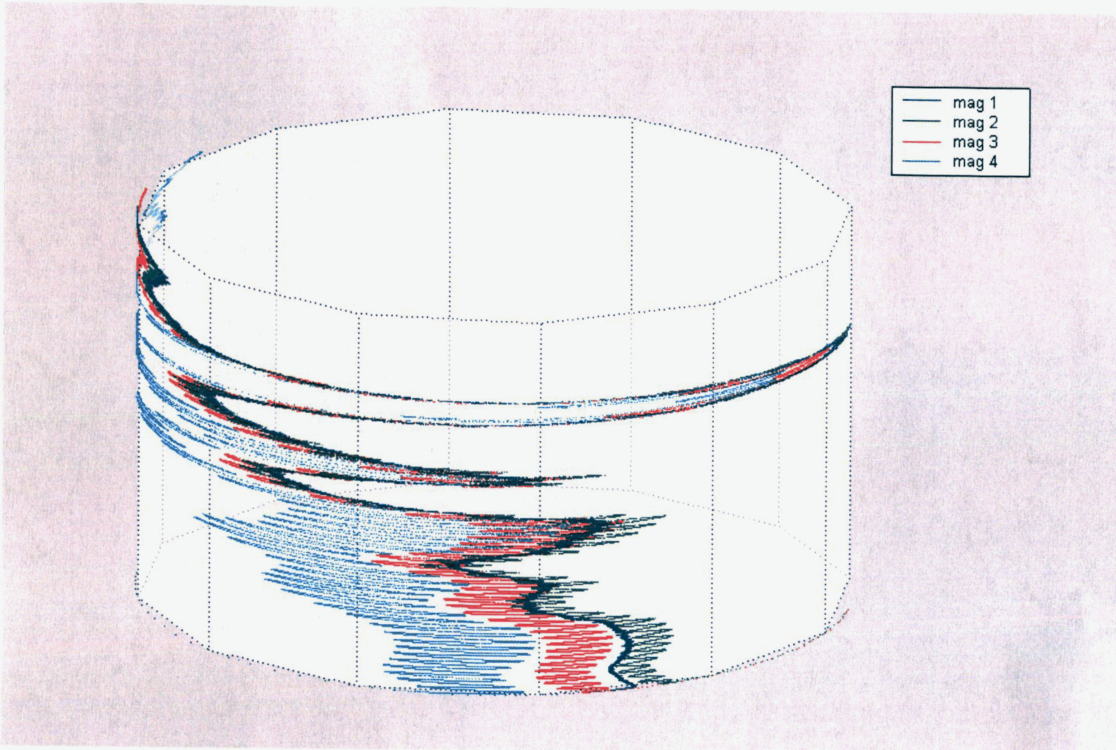

Figure 11. Filtered azimuth signals from four magnetometers from 10000 - 12000 seconds.

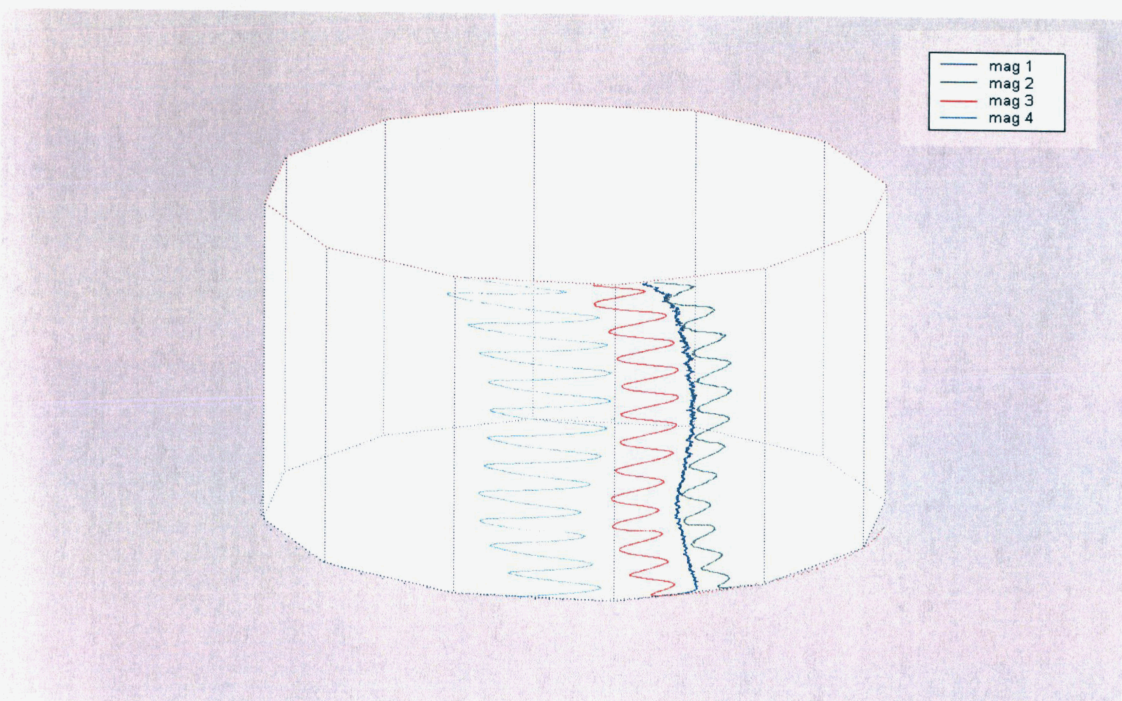

Figure 12. A 400 second section of Figure 11 shows the load train motion dominated by a 33 second period oscillation plus a longer period 300 second oscillation.

Concluding Remarks

The intent has been to show how basic attitude measurements can illustrate much about the nature of the balloon, load train, and gondola dynamics. It is evident that magnetometers can detect the rotation of the load train at different stations giving a picture of its azimuth dynamics, while data from rate and integrated-rate gyros can simultaneously detect elevation and cross elevation performance. The set of data of presented in this paper is for one flight only. Analysis of the results and modeling of the load train dynamics are topics for future study and have not been addressed here. On a future flight, augmenting the sensors discussed here with GPS position sensors not only on the gondola, but at stations along the ladder and close to the balloon might provide a clearer picture of the effects of aerodynamic excitation. The real-time prediction of these disturbances would be a significant step toward improving the pointing accuracies and flight opportunities for stratospheric balloons.

Further Reading:

"Typical Flight Train D-400,271" drawing by the National Scientific Balloon Facility, 1984.

"A Balloon_Borne Millimeter-Wave Telescope for Cosmic Microwave Background Anisotropy Measurements", Fixsen, D. J. et al, The Astrophysical Journal, 470: 63 –77, 1996 October 10.

"A Solar Pointing System for the Long Duration Balloon Missions", Hanagud, J. M. et al, AIAA-97-1516, 1997.

"Linear-Quadratic-Regulator Pointing Control System for a High-Altitude Balloon Payload", White, John E. and Etter, Jerry Etter, pp 615-623, J. Guidance, Vol 13, No. 4. July-August 1990.

"On the Nature of Vertical Oscillations of Constant Volume Balloons", Massman, William J., 1351-1355, Journal of Applied Meteorology, September, 1978.

Appendix Balloon Measurements

Appendix: Measurements

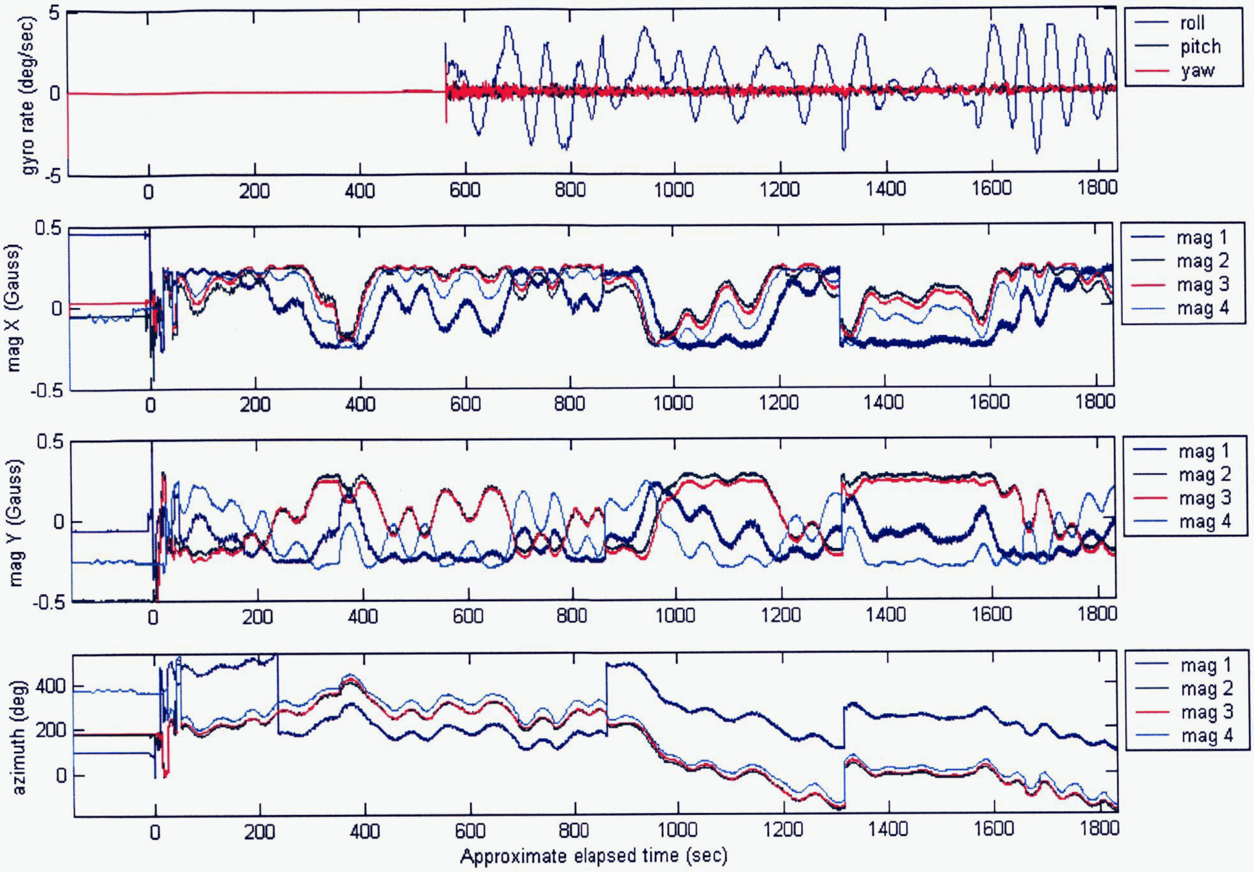

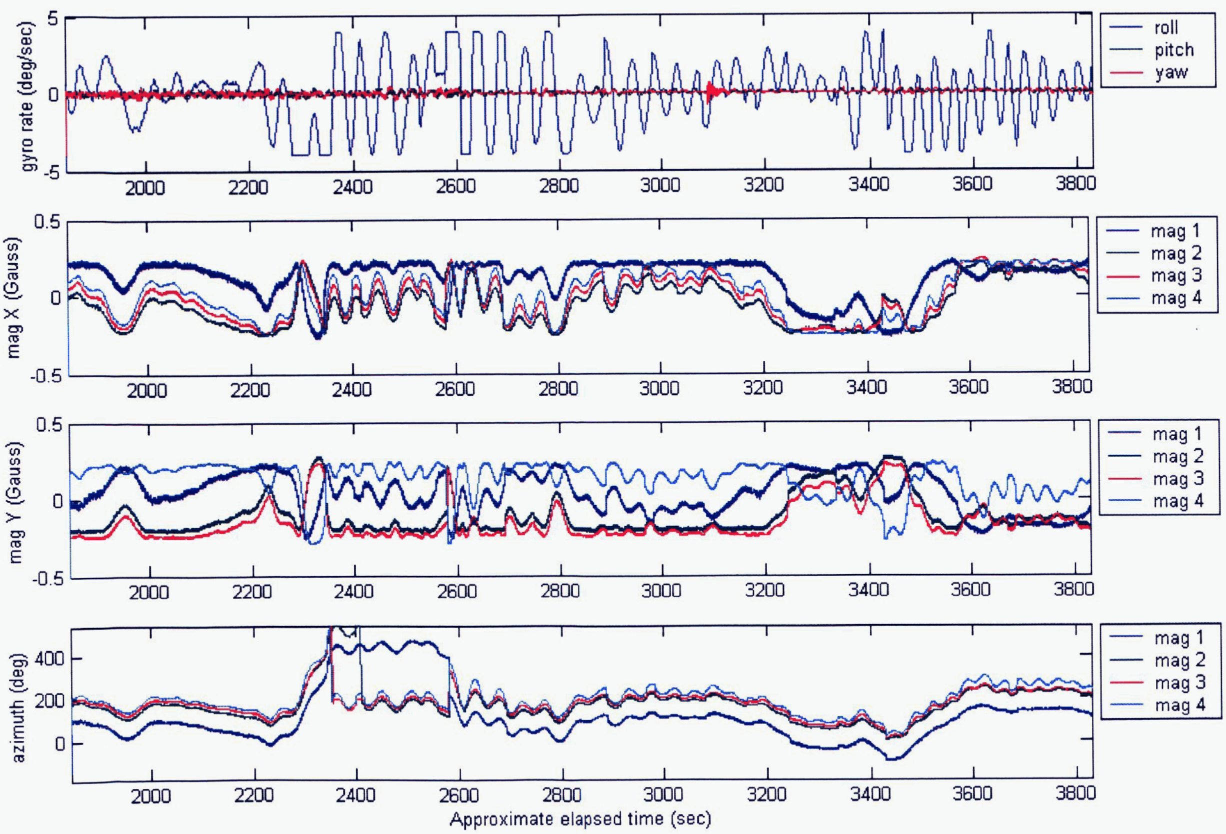

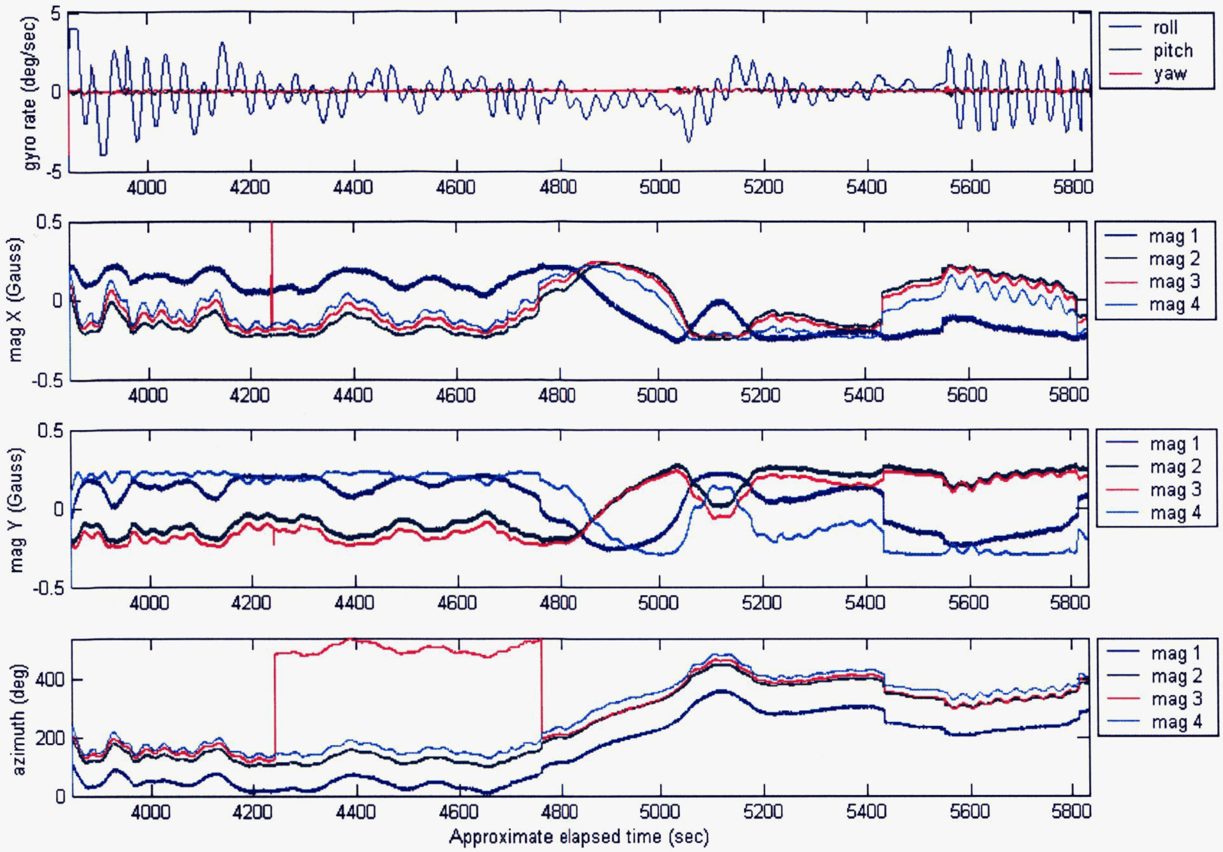
gyro rate (deg/sec)
roll
pitch
yaw
mag X (Gauss)
mag Y (Gauss)
azimuth (deg)
mag 1
mag 2
mag 3
mag 4
Approximate elapsed time (sec)

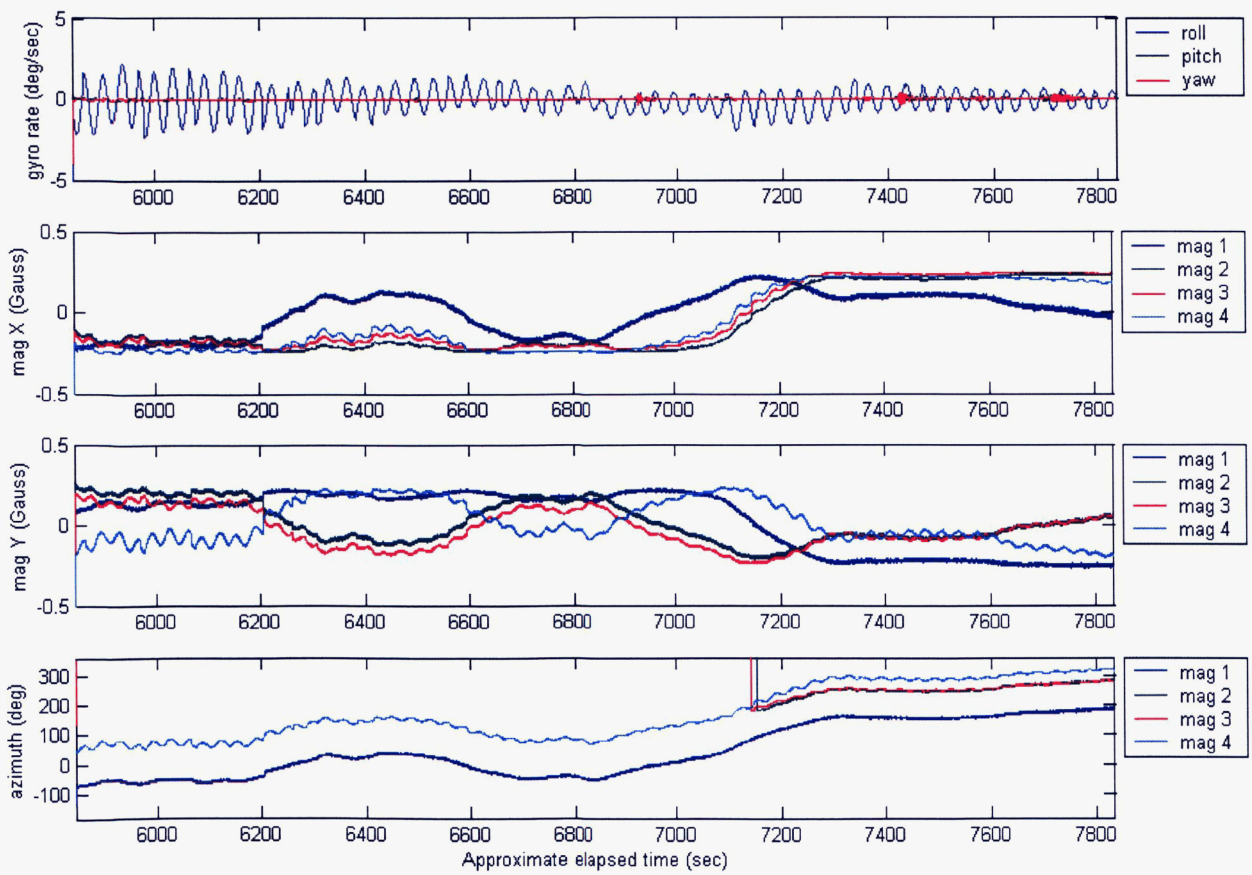
gyro rate (deg/sec)
roll
pitch
yaw
mag X (Gauss)
mag Y (Gauss)
azimuth (deg)
mag 1
mag 2
mag 3
mag 4
Approximate elapsed time (sec)

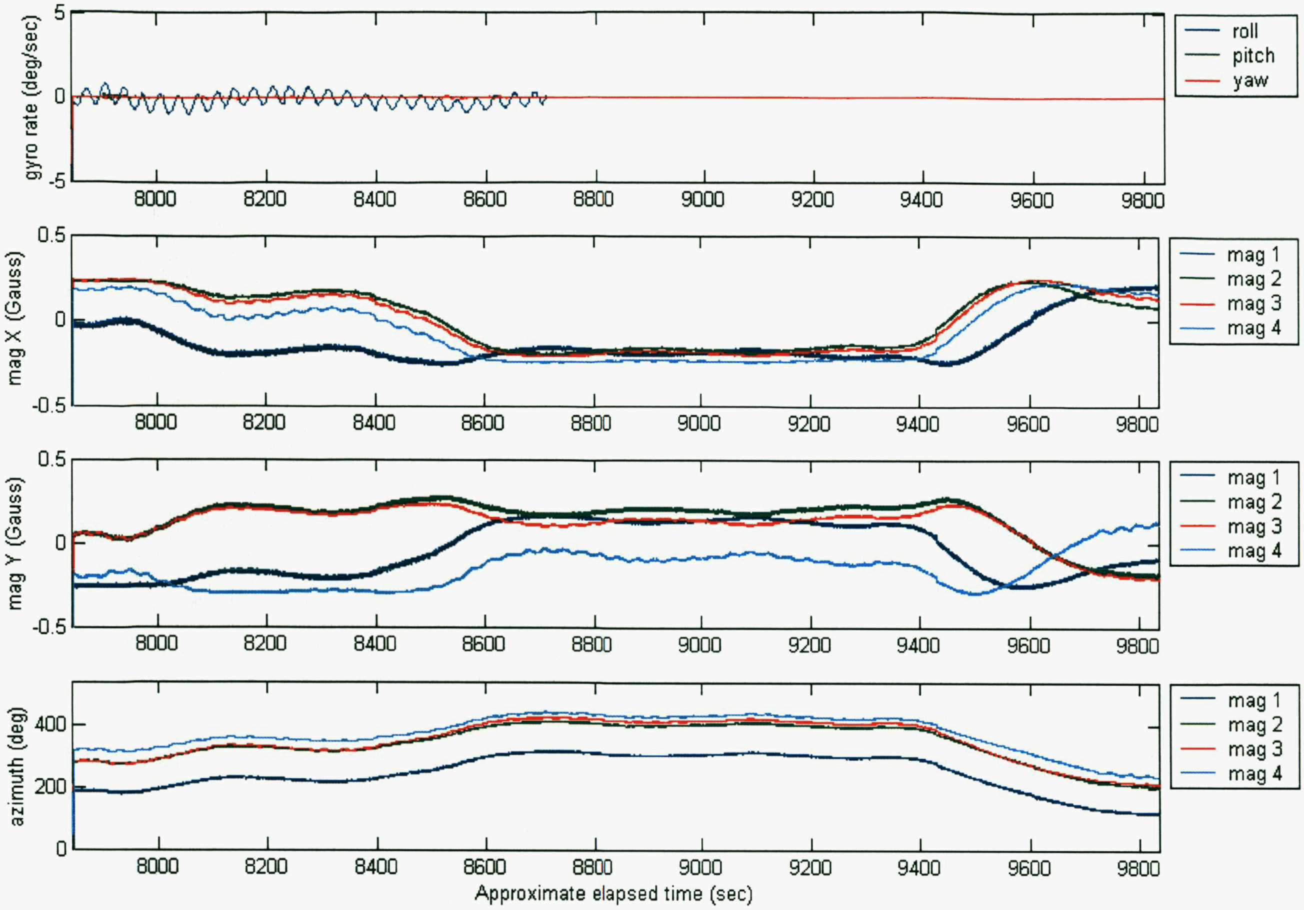

gyro rate (deg/sec)
roll
pitch
yaw
mag X (Gauss)
mag Y (Gauss)
azimuth (deg)
mag 1
mag 2
mag 3
mag 4
8000 8200 8400 8600 8800 9000 9200 9400 9600 9800
Approximate elapsed time (sec)

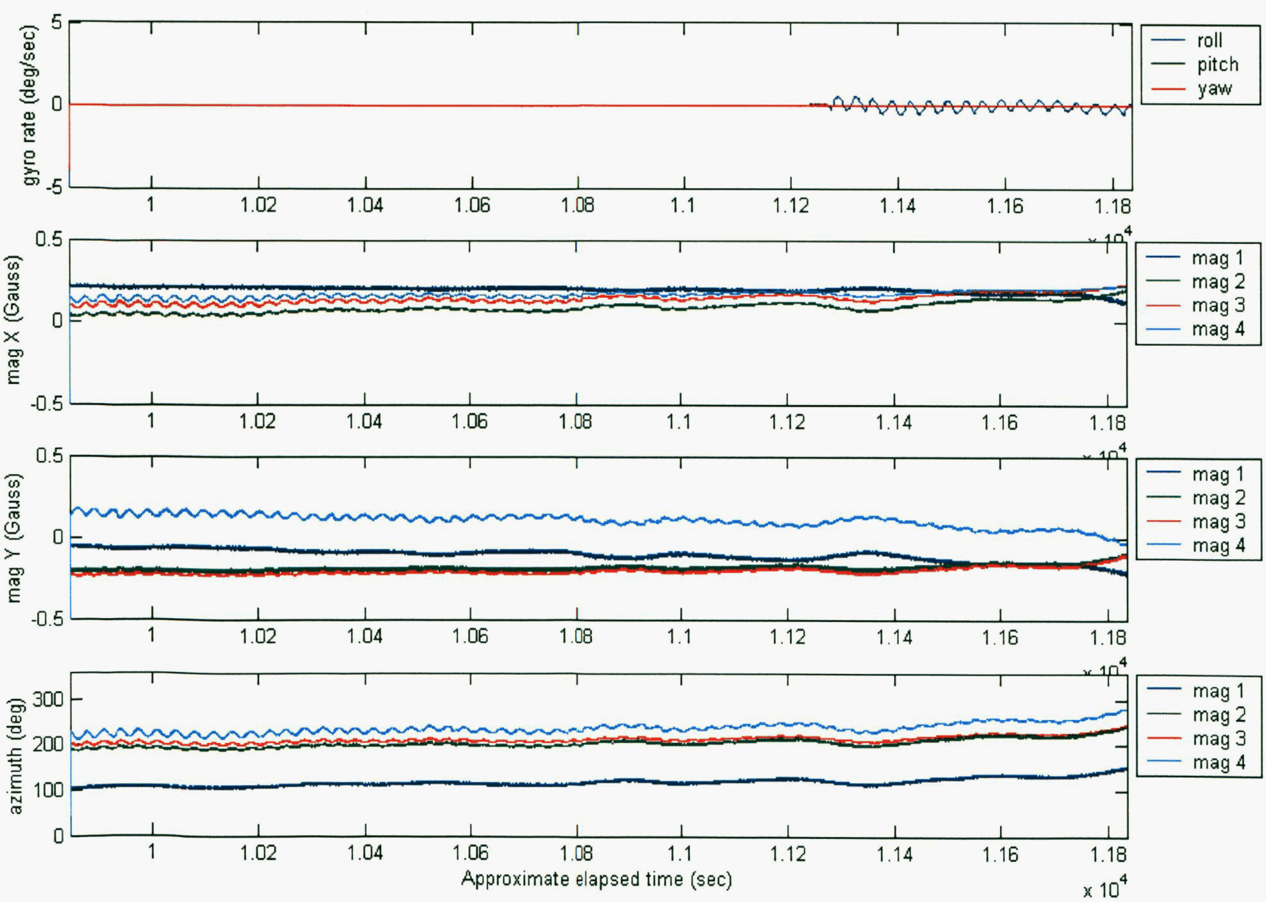

gyro rate (deg/sec)
roll
pitch
yaw
mag X (Gauss)
mag Y (Gauss)
azimuth (deg)
mag 1
mag 2
mag 3
mag 4
1 1.02 1.04 1.06 1.08 1.1 1.12 1.14 1.16 1.18
x 10^4
Approximate elapsed time (sec)

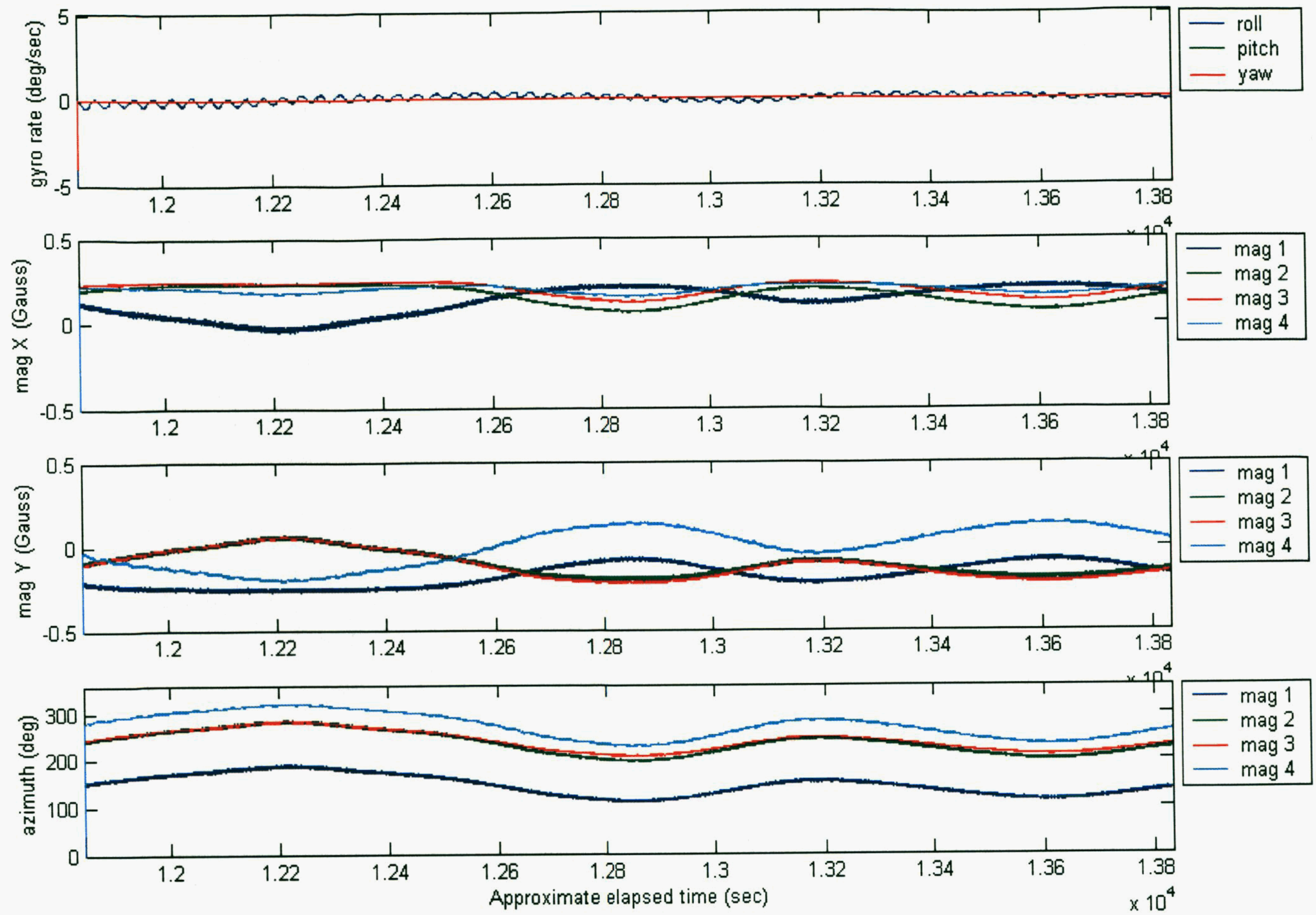

gyro rate (deg/sec)
roll
pitch
yaw
mag X (Gauss)
mag Y (Gauss)
mag 1
mag 2
mag 3
mag 4
azimuth (deg)
1.2 1.22 1.24 1.26 1.28 1.3 1.32 1.34 1.36 1.38
Approximate elapsed time (sec)
x 10^4

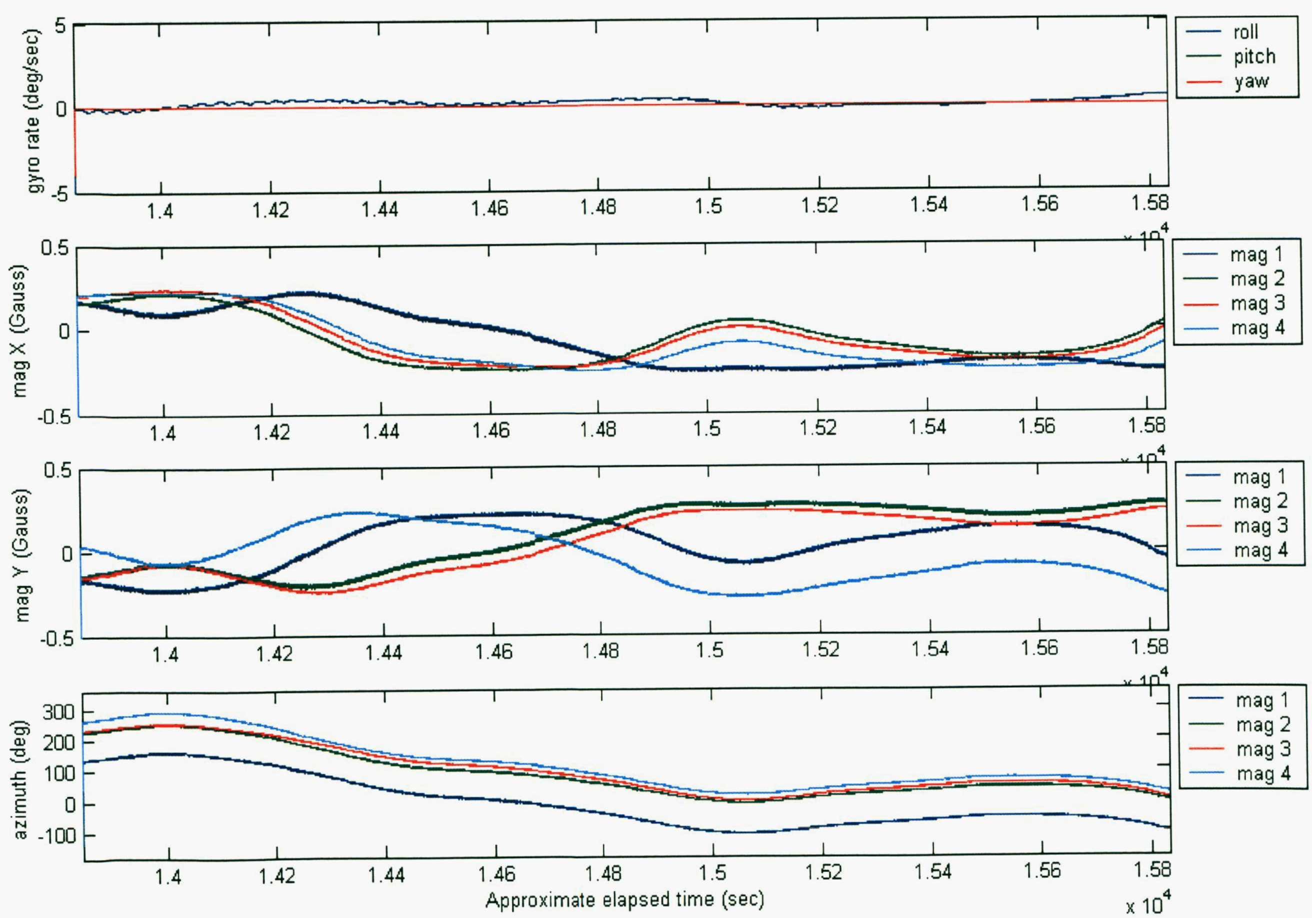

gyro rate (deg/sec)
roll
pitch
yaw
mag X (Gauss)
mag Y (Gauss)
mag 1
mag 2
mag 3
mag 4
azimuth (deg)
1.4 1.42 1.44 1.46 1.48 1.5 1.52 1.54 1.56 1.58
Approximate elapsed time (sec)
x 10^4

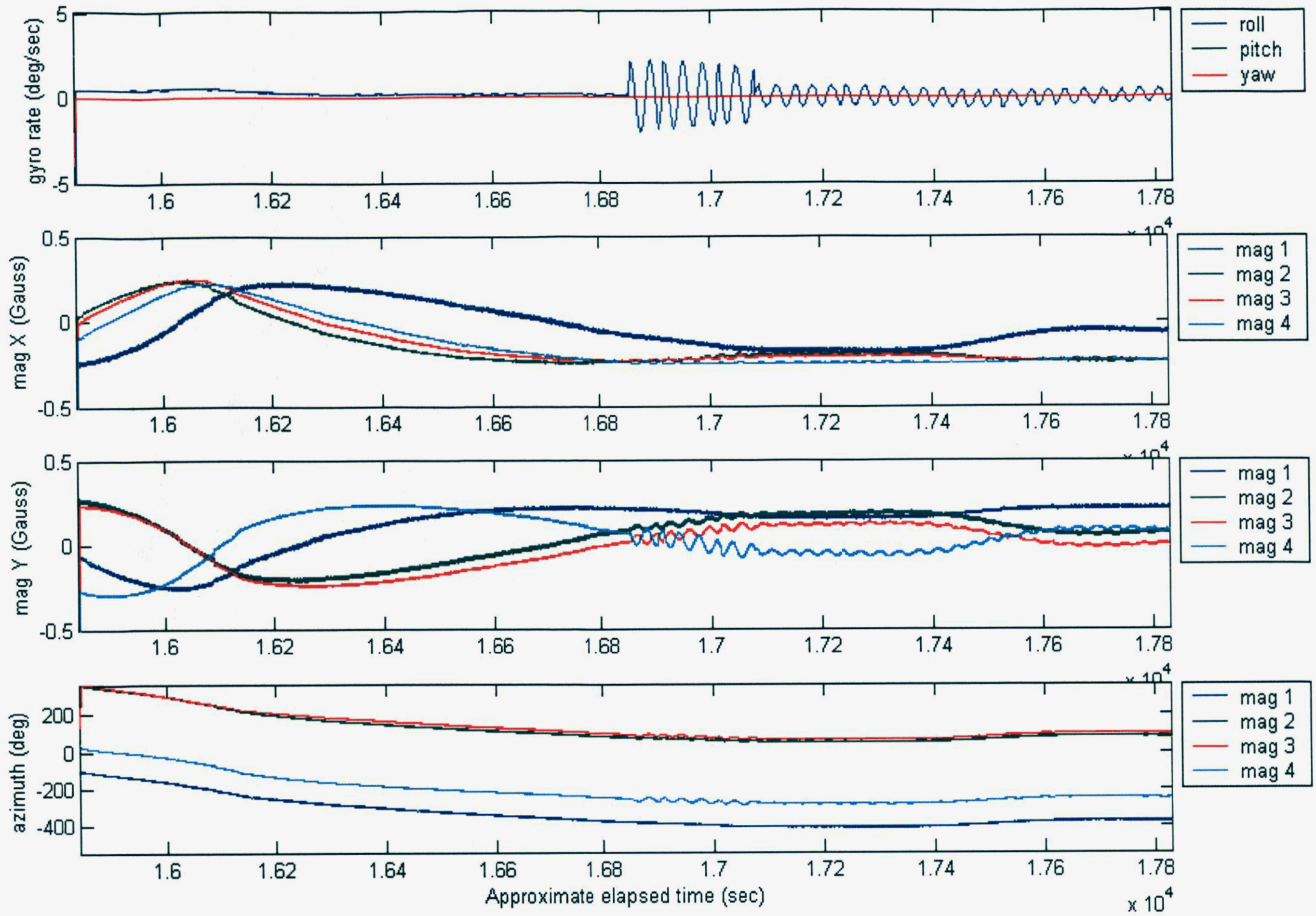
gyro rate (deg/sec)
roll
pitch
yaw
mag X (Gauss)
mag Y (Gauss)
azimuth (deg)
mag 1
mag 2
mag 3
mag 4
1.6 1.62 1.64 1.66 1.68 1.7 1.72 1.74 1.76 1.78
Approximate elapsed time (sec)
x 10^4

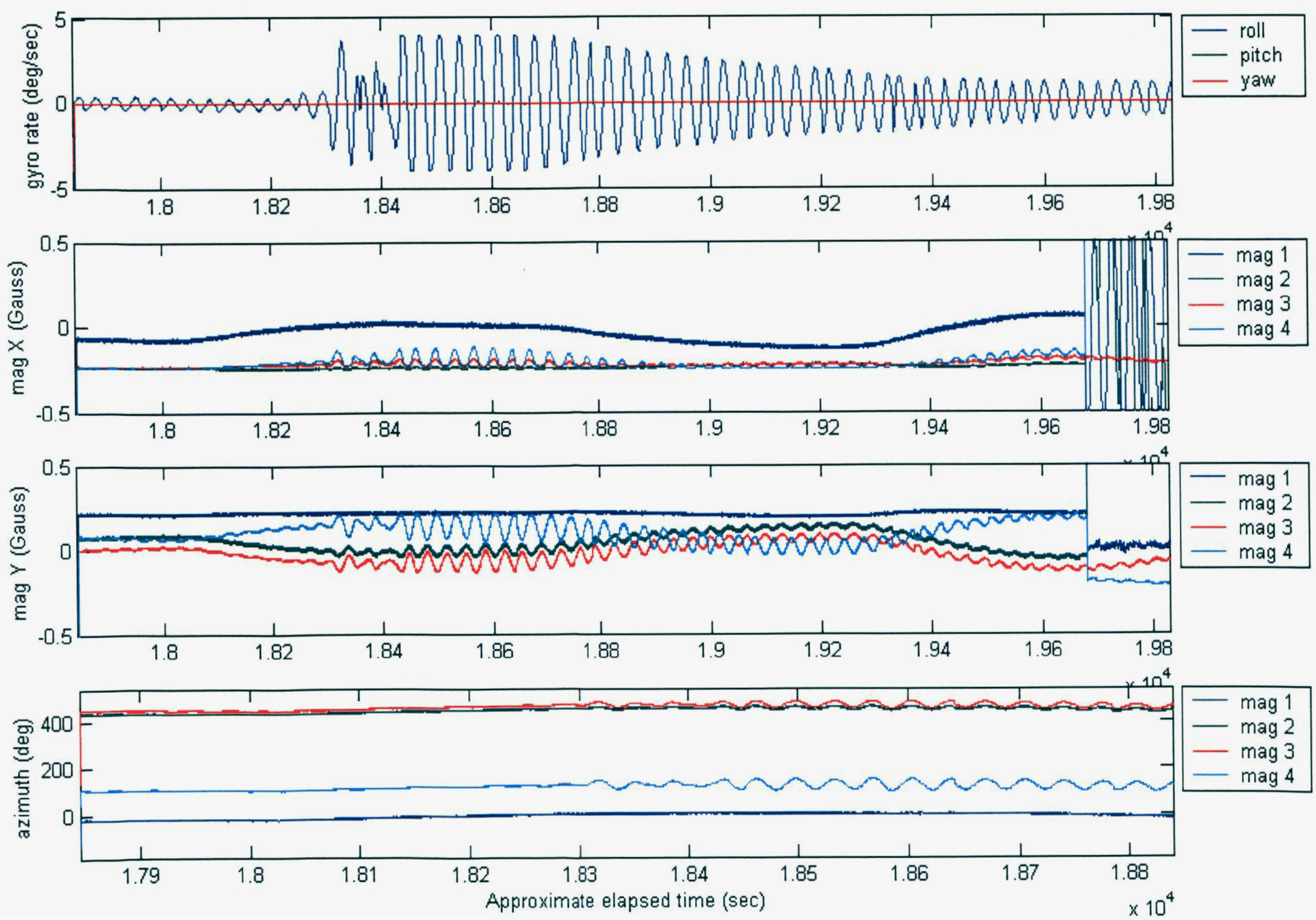
gyro rate (deg/sec)
roll
pitch
yaw
mag X (Gauss)
mag Y (Gauss)
azimuth (deg)
mag 1
mag 2
mag 3
mag 4
1.8 1.82 1.84 1.86 1.88 1.9 1.92 1.94 1.96 1.98
1.79 1.8 1.81 1.82 1.83 1.84 1.85 1.86 1.87 1.88
Approximate elapsed time (sec)
x 10^4